# Unsteady Subsonic Aerodynamic Loadings Caused by Control Surface Motions

W. S. Rowe,* B. A. Winther†, and M. C. Redman‡
*Boeing Commercial Airplane Company, Renton, Wash.*

**A numerical method is presented for the prediction of unsteady aerodynamic loadings on lifting surfaces that are due to oscillations of trailing edge control surfaces having sealed gaps in subsonic compressible flow. The development is applicable to planform configurations having full span or multiple partial span control surfaces located anywhere along the planform trailing edge. The final form of the downwash integral equation is formulated by separating the singular terms from the non-singular terms of the integral equation. A systematic solution process is developed to remove and separately evaluate the discontinuities in the kinematic downwash distribution. A suggestion is made for modifying the boundary conditions to include local velocities due to airfoil thickness effects within the solution process. Comparisons of theoretical and experimental pressure data indicate that reasonably accurate pressure distributions may be obtained for a wide range of control surface configurations.**

## Nomenclature§

| | | |
|---|---|---|
| $b_0$ | = | reference length |
| $H_j(x,y)$ | = | mode shape of mode $j$ |
| $i$ | = | $(-1)^{1/2}$ |
| $K(x,\xi,y,\eta)$ | = | kernel function, Eq. (4) |
| $k$ | = | reduced frequency = $\omega b_0/V$ |
| $M$ | = | Mach number |
| $P_l$ | = | pressure on lower surface, [force/area] |
| $P_u$ | = | pressure on upper surface, [force/area] |
| $q_j$ | = | generalized coordinate amplitude for mode $j$ |
| $s$ | = | nondimensional semispan, $S/b_0$ |
| $V$ | = | freestream velocity, [length/time] |
| $\bar{w}/V$ | = | kinematic angle of attack or nondimensional normalwash |
| $x,y,z$ | = | coordinates nondimensional with respect to $b_0$ |
| $\beta$ | = | $(1-M^2)^{1/2}$ |
| $\rho$ | = | density of the fluid [mass/length$^3$] |
| $t$ | = | time |
| $\omega$ | = | circular frequency of oscillation [1/time] |

## Introduction

Historically, numerical methods developed to predict the unsteady loadings due to control surface motions have been formulated using the kernel function approach. Differences between various methods exist mainly in the manner in which the pressures are assumed to be distributed over the surface and in the way in which solution accuracy is maintained.

A relatively successful program was developed earlier in an attempt to devise a single procedure that may be used to handle a general class of nonplanar problems which would not require user foreknowledge of the behavior of the final pressure distribution in regions of downwash discontinuities. The method is based on the vortex-lattice technique in which the surface is idealized as a set of lifting elements that are modeled as short line segments of acceleration-potential doublets.[1] The load on each element is determined by satisfying normal velocity boundary conditions at a set of control points distributed over the surface. However, considerable variation in results may be obtained depending upon the method used to define the control point distribution. It appears that results will approach asymptotic values provided that a sufficiently large number of control points are used. Asymptotic values may also be approached using a smaller number of control points provided that the points are distributed in a fashion that resembles the distribution of integration stations defined by integration quadrature formulas used in the numerical evaluation of functions having singular characteristics. Therefore, in using a small number of control points in order to obtain computer efficiency, the analyst must have knowledge of the various types of singularities existing in the final pressure distribution before the control point distribution can be artfully selected to obtain a converged solution.

Methods developed using the traditional approach of combining analytically defined pressure distribution functions to satisfy the surface boundary conditions also require prior knowledge of the behavior of the final pressure distribution. In this approach the responsibility for obtaining converged solutions is placed more on the program developer rather than on the program user.

Foreknowledge of only the final pressure distribution behavior may still prove to be an insufficient criteria in developing solutions that are insensitive to the distribution and number of control points used in the analysis. The work of Ref. 2 is one of the few subsonic methods developed around the assumed pressure mode approach using pressure terms that are capable of correctly representing the known singularity functions around the boundaries of the control surface. However, the resulting solutions are also sensitive to the relative location and number of control point collocation stations used in the analysis. The sensitivity may be attributed to the particular solution process being applied that assumes that discontinuous and continuous downwash distributions may be combined to satisfy the boundary conditions at a select set of control points. Changing the control point locations by relatively small amounts results in large changes in the unsteady loadings, consequently, the method requires calculation of downwashes at many stations and seeking solutions in a least-squares-error sense.

Presented as Paper 73-315 at the AIAA Dynamics Specialists Conference, Williamsburg, Va., March 19-20, 1973; submitted April 19, 1973; revision received October 10, 1973. This research was supported in part by NASA Contract NAS1-10536 and in part by Boeing IR&D Program.

Index categories: Nonsteady Aerodynamics; Subsonic and Transonic Flow.

*Research Specialist.

†Research Engineer. Member AIAA.

‡Engineer.

§ Dimensionless quantities except as noted.

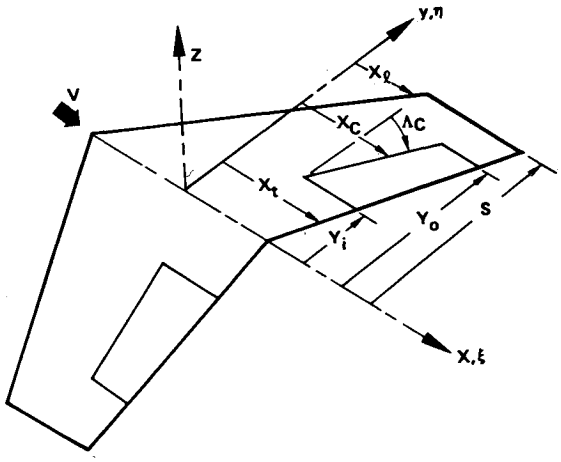


**Fig. 1 Coordinate system definition.**

It appears that solution sensitivity may be reduced provided that the downwash discontinuities are removed from the kinematic downwash distribution prior to applying the direct lifting surface solution process. However, the added step requires an analytical formulation of the pressure expression having known strengths that will produce downwash discontinuities having the same values as contained in the kinematic distribution. Pressure expressions meeting these requirements have been developed by Landahl[3] for the inboard partial span control surface case and by Ashley and Rowe[4] for the case of a control surface that extends to the planform side edge.

The present work represents an extension of the analytical methods suggested by Landahl[3] to provide a capability of predicting unsteady loadings caused by control surface motion that is relatively insensitive to the distribution and number of control stations placed on the lifting surface.

## Elements of the Integral Equation

The analytical formulation has been developed for analysis of planform configurations having full span or multiple partial span control surfaces located anywhere along the planform trailing edge.

The analytical coordinate system is defined for a typical partial span control surface configuration shown in Fig. 1.

The expression for the lifting surface downwash-pressure relationship derived by Kussner[5] provides the basis for formulating the downwash-integral equation in the following form:

$$\left[\frac{\bar{w}}{V}\right]_j = \frac{1}{4\pi\rho V^2}\int_{-s}^{s}\int_{x_t}^{x_t} \Delta P_j(\xi,\eta)K(x,\xi,y,\eta)d\xi d\eta \quad (1)$$

The pressure distribution $\Delta P_j(\xi,\eta)$ is the only unknown function within the equation and is equal to the pressure difference between lower and upper surfaces defined by $\Delta P_j(\xi,\eta) = P_l - P_u$

The kinematic downwash term $[\bar{w}/V]_j$ is developed on the basis of the modal representation of the wing deflection $Z$ for sinusoidal motion

$$Z = \sum_j H_j(x,y)q_j e^{i\omega t} \quad (2)$$

and is defined as

$$\left[\frac{w}{V}\right]_j = \left[\frac{\bar{w}}{V}\right]_j q_j e^{i\omega t} =$$

$$-\left[\frac{\partial H_j(x,y)}{b_0\partial x} + i\,\frac{\omega}{V}H_j(x,y)\right]q_j e^{i\omega t} \quad (3)$$

where $H_j(x,y)$ is the deflection shape of the $j$th mode and is in the same dimensional units as $b_0$ and $q_j$ is dimensionless.

The subscript $(j)$ is omitted in the remaining sections with the understanding that the pressure terms being determined are those terms necessary to satisfy the $j$th mode shape boundary conditions.

The $K(x,\xi,y,\eta)$ term represents the kernel function of the integral equation that describes the surface normalwash at $(x,y)$ due to a pulsating pressure doublet located at $(\xi,\eta)$. The kernel function[5] has been reduced to a form that may be easily evaluated by routine numerical procedure by Watkins, Runyan, and Woolston[6] and presented in a nondimensional form as

$$K(x,\xi,y,\eta) =$$

$$= \frac{e^{-ikx_0}}{y_0^2}\left\{-k|y_0|\left[K_1|ky_0| + i\frac{\pi}{2}(I_1|ky_0| - L_1|ky_0|) - i\right.\right.$$

$$\left. -i\int_0^h \tau/(1+\tau^2)^{1/2}\exp(ik|y_0|\tau)d\tau\right]$$

$$\left. -x_0/(x_0^2+\beta^2y_0^2)^{1/2}\cdot\exp\frac{ik}{\beta^2}(x_0 - M(x_0^2+\beta^2y_0^2)^{1/2})\right\} \quad (4)$$

where

$$h = (x_0 - M(x_0^2+\beta^2y_0^2)^{1/2})/\beta^2y_0;\ x_0 = x-\xi;\ y_0 = y-\eta$$

Singularities contained in Eq. (4) have been identified and are isolated in the following form:

$$K(x,\xi,y,\eta) = K_{ns}(x,\xi,y,\eta) + K_s(x,\xi,y,\eta) \quad (5)$$

where $K_{ns}(x,\xi,y,\eta)$ is the nonsingular part of the kernel function.

The singular part is given by

$$K_s(x,\xi,y,\eta) =$$

$$= e^{-ikx_0}\left\{-\frac{1}{y_0^2}[1 + x_0/(x_0^2+\beta^2y_0^2)^{1/2}] + \right.$$

$$ik/(x_0^2+\beta^2y_0^2)^{1/2}$$

$$-\frac{k^2}{2}\ln|(x_0^2+\beta^2y_0^2)^{1/2} - x_0| -$$

$$\left.\frac{k^2}{2\beta^2}[x_0/(x_0^2+\beta^2y_0^2)^{1/2} - M]\right\} \quad (6)$$

This expression contains the dipole, inverse square root, and logarithmic singularities identified in Ref. 6. The last term of Eq. (6) is not singular but is included since special means are required in evaluating the downwashes due to this term in regions near the downwash chord.

Insertion of the above definitions into the downwash integral equation results in the following expression to be evaluated over the surface to satisfy the boundary conditions.

$$4\pi\rho V^2\left[\frac{\bar{w}}{V}\right] =$$

$$= \int\int\Delta p(\xi,\eta)K_{ns}(x,\xi,y,\eta)d\xi d\eta + \int\int\Delta p(\xi,\eta)K_s(x,\xi,y,\eta)d\xi d\eta \quad (7)$$

### Evaluation of the Dipole Term

The downwash contribution due to the dipole term is evaluated using the method suggested by Hsu.[7] The dipole integral is given as

$$\bar{W}^{dp} =$$

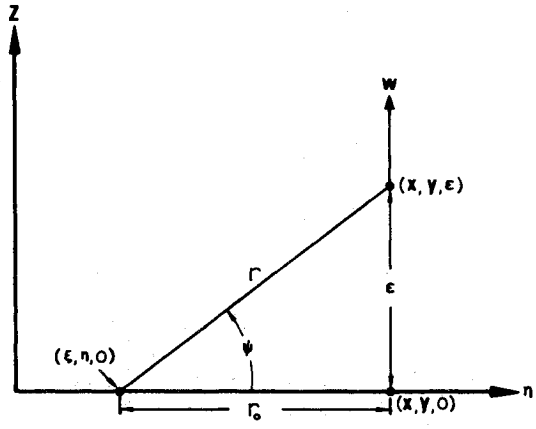


**Fig. 2 Dipole coordinate system.**

$$= -\int_{-s}^{s}\int_{x_l}^{x_t} \Delta p(\xi,\eta) e^{-ikx_0} \frac{1}{(y-\eta)^2}[1 + (x-\xi)/[(x-\xi)^2 + (y-\eta)^2]^{1/2}]d\xi d\eta \quad (8)$$

Downwash contribution due to the dipole portion of the kernel function is accomplished by considering the normalwash at a point $(x,y,\epsilon)$ that is located just off of the surface shown in Fig. 2.

The kernel function describing the normalwash at $(x,y,\epsilon)$ due to a pressure pulse at $(\xi,\eta,o)$ is given by

$$K_w = e^{-ikx_0}\left[\frac{1}{r}\frac{\partial E_0}{\partial r} + \sin^2\psi\left(\frac{\partial^2 E_0}{\partial r^2} - \frac{1}{r}\frac{\partial E_0}{\partial r}\right)\right] \quad (9)$$

where

$$E_0 = \int_{-\infty}^{h} e^{ik\lambda}(r^2 + \lambda^2)^{-1/2} d\lambda$$

$h = [x_0 - MR]/\beta^2$, $R = (x_0^2 + \beta^2 r^2)^{1/2}$ and $x_0 = x - \xi$

Using the geometric properties of Fig. 2 given as

$$r^2 = r_0^2 + \epsilon^2;\ r_0 = y_0 = y - \eta \text{ and } \sin\psi = \frac{\epsilon}{r};$$

$$R_0 = (x_0^2 + \beta^2 r_0^2)^{1/2}$$

Then $K_W{}^{dp}$ takes on the definition

$$K_W{}^{dp} = -e^{-ikx_0}\frac{r_0^2 - \epsilon^2}{(r_0^2 + \epsilon^2)^2}\left[1 + \frac{x_0}{R_0} + 0(\epsilon^2)\right] \quad (10)$$

where the terms represented by $0(\epsilon^2) \to 0$ as $\epsilon \to 0$.

The normalwash at $(x,y,0)$ is obtained by a limiting process allowing $\epsilon \to 0$ after the normalwash integral has been evaluated as indicated by the following:

$$W^{dp}(x,y,0) = \lim_{\epsilon\to 0} -\int_{-s}^{s} \frac{(y_0^2 - \epsilon^2)(s^2 - \eta^2)^{1/2}}{(y_0^2 + \epsilon^2)^2}\int_{x_l}^{x_t} \times \frac{\Delta p(\xi,\eta)}{(s^2-\eta^2)^{1/2}} e^{-ikx_0}(1 + \frac{x_0}{R_0})d\xi d\eta \quad (11)$$

Following the development of Ref. 7, let $G(x,y,\eta)$ be the chordwise integral given as

$$G(x,y,\eta) = \int_{x_l}^{x_t} \frac{\Delta p(\xi,\eta)}{(s^2-\eta^2)^{1/2}} e^{-ikx_0}(1 + x_0/R_0)d\xi \quad (12)$$

as $\eta \to y$ this becomes $\lim_{\eta\to y} G(x,y,\eta) = G(x,y,y)$

One of the singularities is then subtracted from Eq. (11) to provide the expression

$$W^{dp}(x,y,0) = \lim_{\epsilon\to 0}\left[-\int_{-s}^{s} y_0 \frac{(y^2-\eta^2)(s^2-\eta^2)^{1/2}}{(y_0^2+\epsilon^2)^2}\left[\frac{G(x,y,\eta) - G(x,y,y)}{(y-\eta)}\right]d\eta + G(x,y,y)\int_{-s}^{s}\frac{(y_0^2-\epsilon^2)(s^2-\eta^2)^{1/2}}{(y_0^2+\epsilon^2)^2}d\eta\right] \quad (12a)$$

The finite part of the second integral is equal to the value of $\pi$. Evaluation of the first integral still needs to be accomplished by the use of Cauchy integrals, however, this can be circumvented by subtracting an additional singularity.

Define

$$H(x,y,\eta) = (s^2-\eta^2)[G(x,y,\eta) - G(x,y,y)]/(y-\eta)$$

$$H(x,y,y) = \lim_{\eta\to y}(s^2-\eta^2)\frac{[G(x,y,\eta) - G(x,y,y)]}{y-\eta} = -(s^2-y^2)G'(x,y,y)$$

adding and subtracting $H(x,y,y)$ provides the form

$$W^{dp}(x,y,0) = \lim_{\epsilon\to 0}\left[-\int_{-s}^{s} y_0 \frac{y_0^2-\epsilon^2}{(y_0^2+\epsilon^2)^2}\frac{1}{(s^2-\eta^2)^{1/2}}\frac{H(x,y,\eta) - H(x,y,y)}{y-\eta}d\eta + H(x,y,y)\int_{-s}^{s} y_0 \frac{y_0^2-\epsilon^2}{(y_0^2+\epsilon^2)^2}\frac{1}{(s^2-\eta^2)^{1/2}}d\eta\right] + \pi G(x,y,y) \quad (12b)$$

The second integral of Eq. (12b) becomes equal to zero as $\epsilon \to 0$ and finally the dipole downwash term takes on the integrable form of

$$W^{dp}(x,y,0) = \int_{-s}^{s}\frac{-1}{(s^2-\eta^2)^{1/2}}\left[(s^2-\eta^2)\frac{G(x,y,\eta) - G(x,y,y)}{(y-\eta)^2} - \frac{(s^2-y^2)G'(x,y,y)}{y-\eta}\right]d\eta + \pi G(x,y,y) \quad (13)$$

It should be noted that, as $\eta \to y$, the integrand of Eq. (13) tends to take on the definition of a second derivative of $G(x,y,\eta)$ with respect to $\eta$. However, the second derivative does not exist since the integrand is singular at the downwash chord $\eta = y$. Figure 3 represents a plot of the span-wise distribution of the integrand $I(y,\eta)$ of Eq. (13) and displays the singularity existing at the downwash chord.

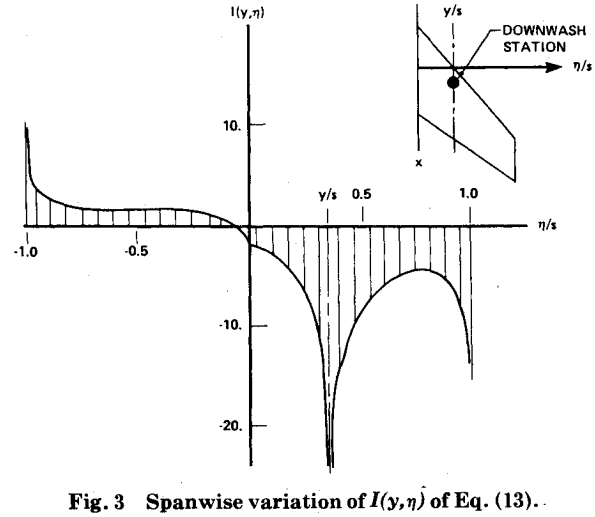


**Fig. 3 Spanwise variation of $I(y,\eta)$ of Eq. (13).**

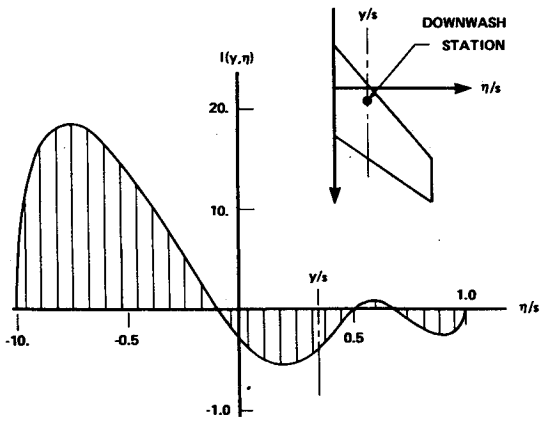


**Fig. 4 Spanwise variation of $I(y,\eta)$ of Eq. (13) with singularities of Eq. (14a) removed.**

### Identification of Spanwise Singularities

The spanwise singularity, observed within the above integral evaluation of the dipole term, was first identified by Multhopp[8] within the development of the steady-state lifting surface solution and has been extended by Laschka[9] for inclusion within the unsteady case.

The functional expression of the dipole singularity may be obtained by developing a Taylor series expansion of $\Delta P(\xi,\eta)e^{-ik\mathbf{x}_0}$ about the downwash station and performing the resulting chordwise integrations. That is, we let $\Delta P(\xi,\eta)e^{-ik\mathbf{x}_0}$ be approximated by the Taylor series given by:

$$\Delta P(\xi,\eta)e^{-ik(x-\xi)} =$$

$$= \left\{\Delta P(x,y) + (\eta - y)\frac{\partial}{\partial\eta}\Delta P(\xi,\eta)_{\substack{\eta=y\\ \xi=x}}\right\} +$$

$$(\xi - x)\left\{\frac{\partial}{\partial\xi}\left[\Delta P(\xi,y)e^{-ik(x-\xi)}\right]\right.$$

$$\left. + (\eta - y)\frac{\partial^2}{\partial\xi\,\partial\eta}\left[\Delta P(\xi,\eta)e^{-ik(x-\xi)}\right]_{\substack{\eta=y\\ \xi=x}}\right\} + \ldots \quad (14)$$

The spanwise singularity expression is identified by insertion of Eq. (14) into the chordwise integral Eq. (12) and performing the integration that results in

$$I^{dp} = -\int_{-s}^{s}\frac{1}{(y-\eta)^2}\left[\left\{\left[\frac{\partial}{\partial\xi}\Delta P(\xi,y)e^{-ik(x-\xi)}\right]_{\xi=x}\right.\right.$$

$$\left.\left. -(y-\eta)\left[\frac{\partial^2}{\partial\xi\,\partial\eta}\Delta P(\xi,\eta)e^{-ik(x-\xi)}\right]_{\substack{\eta=y\\ \xi=x}}\right\}\cdot\right.$$

$$\left.\cdot\left\{\frac{\beta^2}{2}(y-\eta)^2\ln\beta^2(y-\eta)^2\right\} + \text{REGULAR TERMS}\right]d\eta \quad (14a)$$

Thus the dipole term contains the recognizable dipole singularity along with an additional logarithmic singularity at the spanwise downwash station.

The third and fourth integrals of Eq. (7) also contain spanwise singularities that are proportional to $\ln|y-\eta|$ and are identified as

$$I^{(3)}(y) = ik\int_{-s}^{s}\left[\left\{\Delta P(x,y) + (\eta - y)\left[\frac{\partial\Delta P(\xi,\eta)}{\partial\eta}\right]_{\substack{\eta=y\\ \xi=x}}\right\}\cdot\right.$$

$$\left.\cdot\left\{\ln\beta^2(y-\eta)^2\right\} + \text{REGULAR TERMS}\right]d\eta \quad (15)$$

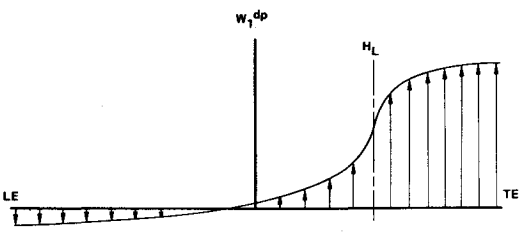


**Fig. 5 Chordwise downwash—singularity ignored.**

$$I^{(4)}(y) = \frac{-k^2}{2}\int_{-s}^{s}\left\{\ln\beta^2(y-\eta)^2\int_{x_1}^{x}\Delta P(\xi,y)e^{-ik(x-\xi)}d\xi +\right.$$

$$\left. + \text{REGULAR TERMS}\right\}d\eta \quad (16)$$

Once the singularities have been determined they may be subtracted out of the integrand and analytically evaluated outside of the integral.

Figure 4 shows the very smooth spanwise distribution of the integrand $I(y,\eta)$ obtained for the dipole term by subtracting out the identifiable singularities of Eq. (14a). Removal of the singularities allows the use of Legendre-Gauss quadrature formulas to evaluate the spanwise integral using only a very small number of quadrature stations.

As a consequence of the above there are several options open to the analyst in evaluating the spanwise portions of the downwash integrals and are 1) ignore the logarithmic singularity since it is of relatively low power, 2) subtract the singularities out of the expression and analytically evaluate their downwash contributions, and 3) apply numerical integration quadrature functions that can evaluate the logarithmic term at the downwash chord.

Numerical investigations have been performed to determine the validity in using any one of the three integration options within the control surface program. The analysis planform is a rectangular wing having a full span flap deflected in steady flow providing a downwash discontinuity value of 1.0 across the hingeline. The assumed pressure distribution used in the analysis is composed of a chordwise singularity term $\ln(\xi - x_c)^2$ and other modifying terms required to produce the discontinuity in downwash across the hingeline as well as satisfying the boundary conditions along the planform edges.

Results of applying option 1) are shown in Fig. 5 where the integral is evaluated using the interdigiting process suggested in Ref. 7, where a single Gauss-Mehler quadrature function is applied over the complete span of the planform. The singularity at the downwash chord is not recognized by this integration procedure and consequently the resulting chordwise downwash distribution is smooth and continuous across the hingeline.

$$W_1^{dp} = \sum_i^I H_i\left[(s^2 - \eta_i^2)\frac{G(x,y,\eta_i) - G(x,y,y)}{(y-\eta_i)^2}\right] + \pi G(x,y,y)$$

Figure 6 presents the results using the second option where the singularity is treated by approximating the

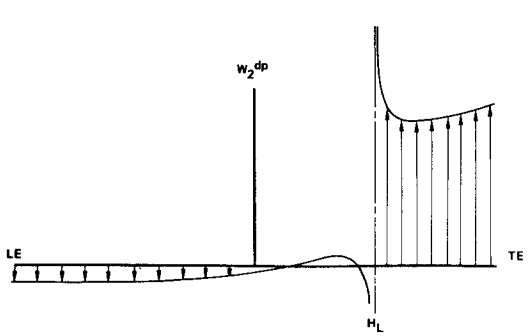


**Fig. 6 Chordwise downwash—singularity subtracted and evaluated separately.**

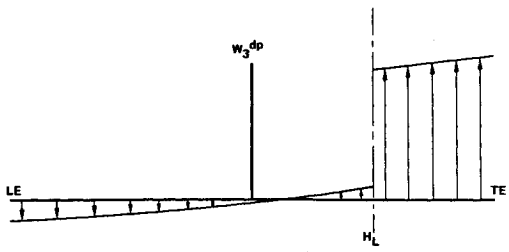


**Fig. 7 Chordwise downwash—singularity evaluated by appropriate quadrature formulas.**

pressure terms by a Taylor series expansion and removing the singularity from the spanwise integrand. Equation (13) has been modified by subtracting the singularities (identified in Eq. (14a)) and evaluating their effect outside of the integral.

The downwash distribution appears to be reasonable at large distances from the hingeline, however, the downwash becomes singular at the hingeline. This is to be expected since the pressure term used in the analysis to provide the step function change in boundary conditions across the hingeline is proportional to $\ln|\xi - x_c|$ which cannot be approximated by a Taylor series in the vicinity of the singularity at $\xi = x_c$.

The downwash distribution indicates that the control stations are to be restricted to chordwise locations that are spaced well away from hingeline where large downwash gradients are developed. This restriction may not be satisfied for analyses of wings having small per cent chord control surfaces. Large gradients may exist over the chordwise length of small percent chord control surface and the resulting solutions would be highly dependent upon the number and relative locations of the downwash collocation stations.

Results of applying option 3) to evaluate Eq. (13) are shown in Fig. 7. The integration interval has been divided into subregions and appropriate quadrature formulas have been applied in the subregions, i.e., square root quadrature formulas applied at ends of the interval, logarithmic quadrature formulas used on either side of the downwash station, and Legendre quadratures applied within the remaining integration intervals.

The resulting downwash distribution does contain the step function change across the hingeline necessary to satisfy the boundary conditions and does not exhibit any large gradients near the hingeline that would cause the solution to be sensitive to the relative locations of the collocation stations.

## Preferred Solution Process

No direct means is available to obtain a closed form solution of the downwash integral equation that satisfies the boundary conditions exactly everywhere on the surface. Approximate solutions are used in lieu of an exact solution process. The approximate solution process is one of generating a finite set of downwash sheets and constructing linear combinations of these sheets to satisfy the boundary conditions at a finite set of preselected control points on the surface.

The downwash sheets are obtained through an evaluation of the downwash integral using assumed pressure distributions that satisfy the required loading conditions on the planform edges.

The assumption usually made is that if the boundary conditions are satisfied at a suitable number of control points distributed over the surface then boundary conditions over the rest of the surface will be satisfied within small error limits.

The approximate procedure is equivalent to assuming that the downwash sheets may be represented by a series of polynomials that are continuous over the surface and may be combined to satisfy the surface boundary conditions at arbitrary control points.

This procedure provides reasonable results for analyses of configurations having continuous downwash distributions, however, it may fail to produce consistently accurate results when applied to analyses of wing-control surface configurations that have discontinuous downwash distributions.

A more systematic solution process applied to the solution of planforms having discontinuous downwash distributions is one of developing a mathematical downwash distribution that has identical discontinuity values that are contained in the kinematic distribution and subtracting this distribution from the original, thus providing a downwash distribution that is continuous over the surface for which the direct lifting surface solution process may be readily applied.

This preferred solution process for discontinuous downwash distributions is given by the matrix equation

$$|W(x,y)| - [\iint \Delta P_s K(\xi,\eta)d\xi d\eta\,]\,a_k \rightarrow |\bar{W}_{\text{mod}}(x,y)|$$

$$|\bar{W}_{\text{mod}}(x,y)| = [\iint \Delta P_r K(\xi,\eta)d\xi d\eta\,]\,|a| \qquad (17)$$

where $\bar{W}_{\text{mod}}(x,y)$ is the continuous downwash distribution obtained by subtracting from the kinematic distribution a distribution having identical values of discontinuities that are contained in the kinematic distribution. $\Delta P_s$ is the singular pressure distributions that provide the same discontinuity characteristics contained in the kinematic downwash distribution. $\Delta P_r$ is the regular pressure distributions used to define continuous downwash distributions.

Use of the preferred solution process requires two pressure distributions to be defined over the lifting surface planform. One of the distributions to provide identical value of downwash discontinuity characteristics as defined by the kinematic downwash distribution and the second pressure function to provide smooth and continuous downwash distributions over the surface.

The pressure distribution resulting from the solution process is the sum of the pressures that provide the discontinuity characteristics and the regular pressure distributions obtained as a solution of modified downwash distribution $\bar{W}_{\text{mod}}(x,y)$.

The key to this solution process is the development of pressure distributions having known strengths that provide identical values of downwash discontinuities contained in the kinematic distribution.

Pressure distributions having known strengths that provide identical discontinuity values of downwash across the boundaries of the control surface have been developed by Landahl[3] for the inboard partial span control surface case and by Ashley[4] for the case of a control surface that extends to the planform side edge.

Landahl obtained a solution that correctly describes the pressure variation near the corner of a nonswept inboard control surface as

$$\bar{P}(\xi,\eta,0) =$$

$$= \frac{-\theta(\eta)}{\pi\beta}\{[1 + 2ik(\xi - x_c)]\ln|((\xi - x_c)^2 + \beta^2(\eta - y_i)^2)^{1/2} - \beta(\eta - y_i)|$$

$$+ [2ik - k^2(\xi - x_c)](\eta - y_i)\ln|((\xi - x_c)^2 + \beta^2(\eta - y_i)^2)^{1/2} - (\xi - x_c)|\} \qquad (18)$$

Equation (18) may be modified to include hingeline sweep effects by defining $\beta$ to take on the following definition:

$$\beta^2 = (1 - M^2 + \tan^2\Lambda)$$

The solution obtained by Ashley[4] for the case of a nonswept control surface having a side edge at the wing tip is given by

$$\bar{C}_p(0) = \frac{\theta(y)}{\pi\beta} \ln \left| \frac{A - [2\beta(s-\eta)]^{1/2}}{A + [2\beta(s-\eta)]^{1/2}} \right| \qquad (19)$$

where $A = [((\xi - x_c)^2 + \beta^2(s-\eta)^2)^{1/2} + \beta(s-\eta)]^{1/2}$

and $\beta$ takes the definition given above for a swept hinge line.

The distribution appears to be correct since $\bar{C}_p(\xi,\eta)$ approaches zero having an infinite slope proportional to the square root of the distance from the wing-tip and also contains a $\ln(\xi - x_c)^2$ term that provides the proper streamwise discontinuity in downwash across the hingeline.

## Loading Functions

The pressure loading functions are defined over the surface only in terms of the pressure loadings caused by motions of the right hand side control surface. For symmetrical control surface deflections, the pressure distributions over the lifting surface due to motions of the left hand side control surface are identical to that of the right hand side, but are reversed left to right, as in a mirror image. Consequently, the complete symmetrical or antisymmetrical loadings may be formulated using only the pressure expression due to motions of the right hand side control surface. This is accomplished for the symmetrical case by defining the total pressure existing at an ($\eta$) station to be the sum of the pressure at ($+\eta$) and those at ($-\eta$) within the pressure expression describing the loadings caused by motions of the right hand side control surface. The total antisymmetrical loadings at an ($\eta$) station are formulated by subtracting the loadings at ($-\eta$) from those at ($+\eta$) within the pressure expression defining loadings caused by motions of the right hand side control surface.

Loading functions are presented here only for the control surface having a side edge at the wing tip and may be easily modified to include the inboard control surface case.

Pressure distributions obtained by the asymptotic expansion process are valid only in localized regions of the planform since the distributions of the outer regions have not been defined nor matched with the inner region solutions. However, the essential part of the pressure distribution that provides the discontinuities in downwash along the control surface edges is defined by the inner region solution. The distribution in the outer regions may take on any convenient form that satisfies the required loading condition along the edges of the planform since a unique distribution is not being determined at this stage of the solution process. Consequently, the surface pressure loading functions that provide the downwash discontinuities are obtained by extending the applicable range of the solutions and modifying these distributions to meet the condition of having the pressures vanish in proportion to the square root of the distance from the edges.

## Loading Functions—Wing Tip Partial-Span Controls

The pressure loading functions for configurations having a control surface side edge at the planform side edge are formulated in the following manner:

$$\Delta P_s(\xi,\eta) = 4\rho V^2(s^2 - \eta^2)^{1/2} f_s(\eta) g_s(\xi,\eta) \qquad (20)$$

where

$$f_s(\eta) = \theta(\eta)/4\pi\beta(s^2 - \eta^2)^{1/2}$$

$$g_s(\xi,\eta) = -g_1(\eta) + k^2(\xi - x_c)g_2(\eta) - 2ik[(\xi - x_c)g_1(\eta) + g_2(\eta)]$$

The $g_1(\eta)$ and $g_2(\eta)$ functions provide symmetric or antisymmetric analysis capability and are defined as

$$g_1(\eta) = g_1{}^R(\eta) + S_F g_1{}^R(-\eta)$$

$$g_2(\eta) = g_2{}^R(\eta) + S_F g_2{}^R(-\eta) \qquad (21)$$

where

$S_F = 1.0$ for symmetric analyses

$S_F = -1.0$ for antisymmetric analyses

The $g_1{}^R(\eta)$ and $g_2{}^R(\eta)$ functions turn on the singularity at the planform side edge and turn it off at the inboard side edge of the control surface at $\eta = y_i$.

$$g_1{}^R(\eta) = e_1(\xi)h_l(\eta) \cdot \ln \left| \frac{A - [2\beta(s-\eta)]^{1/2}}{A + [2\beta(s-\eta)]^{1/2}} \right| - h_r(\eta) \ln \left| [(\xi - x_c)^2 + \beta^2(y_i - \eta)^2]^{1/2} - \beta(y_i - \eta) \right| \} \qquad (22)$$

$$g_2{}^R(\eta) = \beta h_l(\eta) \cdot \{(s-\eta)e_3(\xi,\eta,s)[\ln|[(\xi - x_c)^2 + \beta^2(s-\eta)^2]^{1/2} - (\xi - x_c)| - \ln|[(x_l - x_c)^2 + \beta^2(s-\eta)^2]^{1/2} - (x_l - x_c)|] - h_r(\eta)(y_i - \eta)e_2(\xi,\eta,y_i)[\ln|[(\xi - x_c)^2 + \beta^2(y_i - \eta)^2]^{1/2} - (\xi - x_c)| - \ln|[(x_l - x_c)^2 + \beta^2(y_i - \eta)^2]^{1/2} - (x_l - x_c)|]\} \qquad (23)$$

The $e_1(\xi)$ factor on $g_1{}^R(\eta)$ modifies the chordwise pressure function such that the pressure vanishes at the leading and trailing edge in a square root manner and maintains the required strength at the hingeline to provide the discontinuities across the hingeline.

$$e_1(\xi) = \left[ \frac{(x_t - \xi)(\xi - x_l)}{(x_t - x_c)(x_c - x_l)} \right]^{1/2} \times \left[ 1 - \frac{1}{2}(\xi - x_c)\left( \frac{1}{x_c - x_l} - \frac{1}{x_t - x_c} \right) \right]$$

The $e_{2(}\xi,\eta,y_s)$ factor contained in $g_2{}^R(\eta)$ forces the pressures to vanish having an infinite slope everywhere along the trailing edge except at the control surface side edge where the singularity strengths are maintained to provide the proper change in boundary-condition across the side edge. Using $y_s$ to represent $y_i$ or $y_o$

$$e_2(\xi,\eta,y_s) = \left[ \frac{(x_t - \xi)^2}{(x_t - \xi)^2 + \beta^2(y_s - \eta)^2} \right]^{1/4} \qquad (24)$$

The modifying side edge function $e_3(\xi,\eta,s)$ maintains the proper singularity strength at the side edge and forces the pressure to vanish at the trailing edge with an infinite slope.

$$e_3(\xi,\eta,s) = \left[ \frac{x_t - \xi}{(x_t - \xi) + (s - \eta)} \right]^{1/2} \qquad (25)$$

The $h_l(\eta)$ and $h_r(\eta)$ are the modifying functions that satisfy the planform edge boundary condition while maintaining a second derivative continuity in spanwise loadings and are defined as

$h_l(\eta) =$

$$\begin{cases} 1.0 & \eta \geq -y_i \\ \left[\dfrac{(s-y_i)^2-(y_j+\eta)^2}{(s-y_i)^2}\right]^{1/2}\left[1+\dfrac{1}{2}\dfrac{(y_i-\eta)^2}{(s-y_i)^2}\right] & \eta < -y_i \end{cases}$$

$$h_r(\eta) =$$

$$\begin{cases} \left[\dfrac{(s-y_i)^2-(y_j-\eta)^2}{(s-y_i)^2}\right]^{1/2}\left[1+\dfrac{1}{2}\dfrac{(y_i-\eta)^2}{(s-y_i)^2}\right] & \eta \geq y_i \\ 1.0 & \eta < y_i \end{cases} \tag{26}$$

Insertion of the above loading functions into the downwash integral provides mathematical downwash sheets having identical discontinuity distributions as contained in the kinematic distribution. Subtraction of these downwash sheets from the kinematic distribution results in a modified downwash distribution for which direct solutions may be obtained using a regular lifting surface pressure distribution defined by

$$\Delta P_r(\xi,\eta) = 4\rho V^2(s^2-\eta^2)^{1/2}\sum_m\sum_n a_{nm} f_r^{(n)}(\eta)\cdot g_r^{(m)}(\xi,\eta) \tag{27}$$

where $a_{nm}$ are the unknown coefficient multipliers

$$f_r^{(n)}(\eta) = \frac{\sin(n\phi)}{\sin\phi} \qquad n = \begin{matrix} 1,3,5.\ldots \text{symmetrical} \\ 2,4,6.\ldots \text{antisym-metrical} \end{matrix}$$

$$\phi = \cos^{-1}(\eta/s)$$

$$g_r^{(m)}(\xi,\eta) = \begin{cases} \cot\dfrac{\theta}{2} & m=1 \\ \sin(m-1)\theta & m = 2,3,4,\ldots \end{cases}$$

where the chordwise angular coordinate is defined as

$$\theta = \cos^{-1}\left[-\left(\frac{\xi - x_m(\eta)}{b(\eta)}\right)\right]; \quad x_m(\eta) = \frac{x_t(\eta)+x_l(\eta)}{2}$$

The chordwise angular coordinate $\theta$ is not to be confused with the control surface rotation angle $\theta(y)$.

### Downwash Integral Equation

The downwash-pressure integral equation is formulated using the preferred solution process previously described for evaluating the loadings on lifting surfaces having discontinuous downwash distributions.

The matrix form of the equation is given as

$$4\pi V^2\left[\frac{1}{b_0}\frac{\partial H(x,y)}{\partial x} + ik\frac{H(x,y)}{b_0}\right] - [\iint \Delta P_s(\xi,\eta)K(x,\xi,y,\eta)d\xi d\eta\,] =$$

$$= [\iint \Delta P_r(\xi,\eta)K(x,\xi,y,\eta)d\xi d\eta\,]|a_{nm}| \tag{28}$$

The first matrix on the left hand side represents an array of values defining the kinematic downwash at preselected collocation stations distributed over the surface. The second matrix represents an array of downwashes evaluated at the same stations using a known pressure distribution that provides the same discontinuities that are contained in the kinematic distribution.

The calculated downwash distribution is subtracted from the kinematic distribution to form a modified distribution that is smooth and continuous. Integral equation solutions using the modified distribution as new boundary conditions are obtained by the direct assumed mode solution process.

The spanwise integral on the left hand side is evaluated using logarithmic quadratures in the vicinity of the downwash chord to evaluate the spanwise singularity that has been previously identified. The singularities are removed from the integral on the right hand side and evaluated individually since a meaningful Taylor series expansion may be made for the continuous pressure distributions used in the direct solution process.

The expression defining the mathematical discontinuous downwash distribution represented by the second term on the left hand side of Eq. (28) is given by the following:

$$\int_{-s}^{s}\int_{x_l}^{x_t}\Delta P_s(\xi,\eta)K(x,\xi,y,\eta)d\xi d\eta = \int_{-s}^{s}(s^2-\eta^2)^{1/2}f_s(\eta)\left\{C_s(y,\eta)+C_{ns}(y,\eta) + \frac{f_s(y)}{f_s(\eta)}\left[\frac{C_1^s(y,y)}{(y-\eta)^2} - \frac{s^2-y^2}{s^2-\eta^2}\frac{D_1^s(x,y)}{y-\eta}\right]\right\}d\eta + \Pi f_s(y)C_1^s(y,y) \tag{29}$$

where $C_s(y,\eta)$ and $C_{ns}(y,\eta)$ represent the chordwise integrals due to the singular and nonsingular parts of the kernel function and are given as

$$C_s(y,\eta) = \int_{x_l}^{x_t} g_s(\xi,\eta)K_s(x,\xi,y,\eta)d\xi$$

$$C_{ns}(y,\eta) = \int_{x_l}^{x_t} g_s(\xi,\eta)K_{ns}(x,\xi,y,\eta)d\xi$$

The $C_1^s(y,y)$ and $D_1^s(y,y)$ terms are due to the Hsu integration process where the chordwise integral at $\eta = y$ and the spanwise derivative are removed from the integrand and are defined as

$$C_1^s(y,y) = 2\int_{x_l}^{x} g_s(\xi,\eta)e^{-ik(x-\xi)}d\xi$$

$$D_1^s(x,y) = \frac{f_s'(\eta)_{\eta=y}}{f_s(y)}C_1^s(y,y) + C_2^s(y,y) + r^s(x,y)$$

where

$$C_2^s(y,y) = 2\int_{x_l}^{x} k_s(\xi,y)e^{-ik(x-\xi)}d\xi$$

$$k_s(\xi,y) = \begin{cases} \dfrac{\partial}{\partial\eta}[g_s(\xi,\eta)]_{\eta=y} + e^{-ik(\xi-x_c)}\cdot\dfrac{2\tan\Lambda_c}{(\xi-x_c)} & y_i < \eta < y_0 \\ \dfrac{\partial}{\partial\eta}[g_s(\xi,\eta)]_{\eta=y} & \eta < y_i \end{cases}$$

$$r^s(x,y) = \begin{cases} 0 & \eta < y_i \\ -e^{-ik(x-x_c)}4\tan\Lambda_c \ln\left|\dfrac{x-x_c}{x_l-x_c}\right| & y_i < \eta < y_0 \end{cases}$$

The mathematical continuous downwash distributions represented by the last term of Eq. (28) are evaluated by removing the spanwise singularity from the integrand to produce an integrand that is smooth and continuous and easily evaluated by a few spanwise quadrature terms. The singularities are identified by developing a Taylor series expansion of $\Delta P_r(\xi,\eta)e^{-ik(x-\xi)}$, and performing the chordwise integration as indicated in a previous section.

The expression defining the mathematical continuous downwash distributions represented by the last term of Eq. (28) is given as

$$\int_{-s}^{s}\int_{x_l}^{x_t}\Delta P_r(\xi,\eta)K(x,\xi,y,\eta)d\xi d\eta =$$

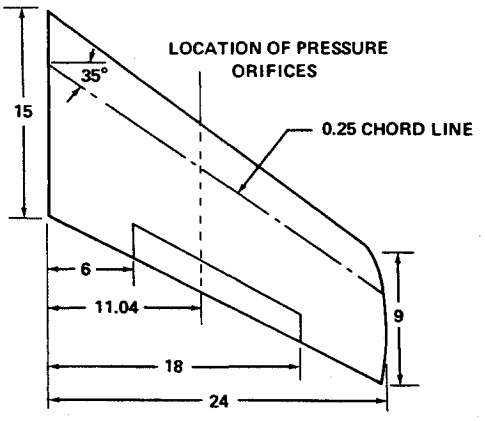


Fig. 8 Experimental planform of NACA RM L53C23 (dimensions in inches).

$$= \int_{-s}^{s} (s^2 - \eta^2)^{1/2} f_r(\eta) \Big\{ C_s{}^r(y,\eta) + C_{ns}{}^r(y,\eta) + \frac{f_r(y)}{f_r(\eta)} \Big[ \frac{C_1{}^r(y,y)}{(y-\eta)^2} - \frac{D_1{}^r(x,y)}{(y-\eta)} - [D_2(x,y) + (y-\eta) D_3(x,y)] \ln \beta^2 (y-\eta)^2 \Big] \Big\} d\eta + \Pi f_r(y) \Big\{ C_1{}^r(y,y) + y D_1{}^r(x,y) + D_2(x,y) \Big[ y^2 + s^2 \Big( \ln \Big| \frac{\beta s}{2} \Big| - \frac{1}{2} \Big) \Big] + D_3(x,y) \Big[ \frac{1}{3} y^3 + y s^2 \cdot \Big( \ln \Big| \frac{\beta s}{2} \Big| - \frac{1}{2} \Big) + y s^2 \Big] \Big\}$$

The subscript $r$ denotes that smooth and continuous pressure distributions are being used in this integral evaluation.

$C_s{}^r(y,\eta)$ and $C_{ns}{}^r(y,\eta)$ represents the chordwise integrals due to the singular and nonsingular parts of the kernel function.

$$C_s{}^r(y,\eta) = \int_{x_l}^{x_t} g_r(\xi,\eta) K_s(x,\xi,y,\eta) d\xi$$

$$C_{ns}{}^r(y,\eta) = \int_{x_l}^{x_t} g_r(\xi,\eta) K_{ns}(x,\xi,y,\eta) d\xi$$

where $g_r(\xi,\eta)$ are the regular lifting surface pressure distributions.

The $C_1{}^r(y,y)$ and $D_1{}^r(x,y)$ terms are due to the Hsu singularity subtracting process and defined as

$$C_1{}^r(y,y) = 2 \int_{x_l}^{x_t} g_r(\xi,\eta) e^{-ik(x-\xi)} d\xi$$

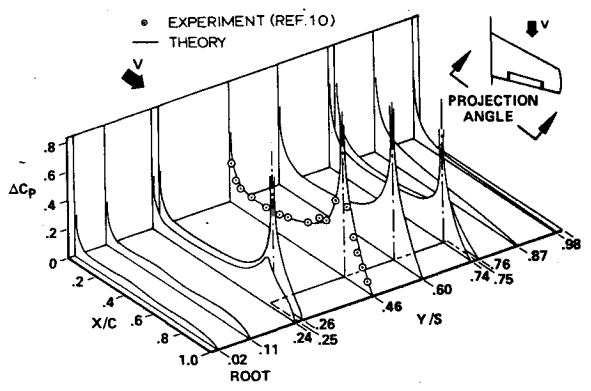


Fig. 9 Chordwise pressure distributions for partial-span flap deflected by $\delta = 10°$, $\alpha = 0°$ at $M = 0.60$ and $k = 0$.

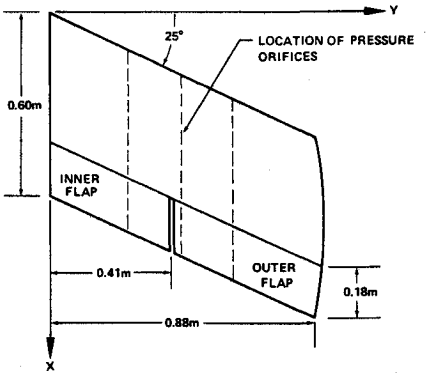


Fig. 10 Experimental planform of Ref. 11 (dimensions in meters).

$$D_1{}^r(x,y) = \frac{f_s{}'(\eta)_{\eta=y}}{f_s(\eta)} C_1{}^r(y,y) + C_2{}^r(y,y) + r_r(x,y)$$

where

$$C_2{}^r(y,y) = 2 \int_{x_l}^{x} k_r(\xi,y) e^{-ik(x-\xi)} d\xi$$

$$k_r(\xi,y) = \begin{cases} \frac{\partial}{\partial \eta} [g_r(\xi,\eta)]_{\eta=y} - \frac{e^{-ik(\xi - x_l)}}{2} \cdot \frac{\partial x_l}{\partial \eta} \cdot \frac{(x_t - \xi)^{1/2}}{(\xi - x_l)^{3/2}} & m = 1 \\ \frac{\partial}{\partial \eta} [g_r(\xi,\eta)]_{\eta=y} & m > 1 \end{cases}$$

$$r_r(x,y) = \begin{cases} -e^{-ik(x-x_l)} \frac{\partial x_l}{\partial \eta} \Big[ \frac{\Pi}{2} + \arcsin \Big( \frac{2x - (x_t + x_l)}{2b(y)} \Big) + 2 \Big( \frac{x_t - x}{x - x_l} \Big)^{1/2} \Big] & \\ 0 & m > 1 \end{cases}$$

The $D_2(x,y)$ and $D_3(x,y)$ terms are due to subtracting the spanwise logarithmic singularities from the integrand and are defined as

$$D_2(x,y) = \frac{\beta^2}{2} \frac{\partial}{\partial \xi} [g_r(\xi,y) e^{-ik(x-\xi)}]_{\xi=x} - ikg_r(x,y) - \frac{k^2}{4} C_1{}^r(y,y)$$

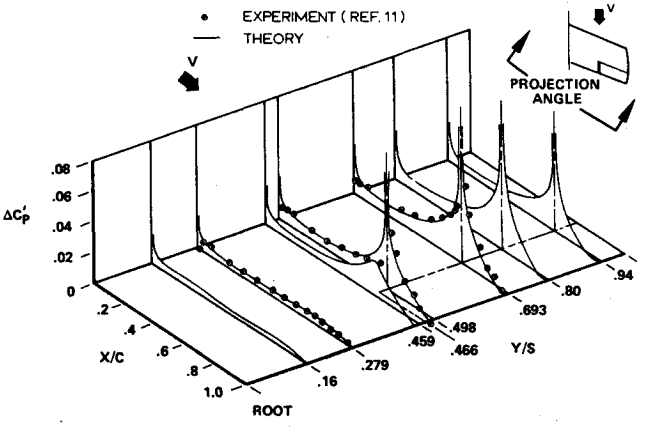


Fig. 11 In-phase chordwise pressure distributions ($A_{i.f.} = 0°$, $A_{o.f.} = 0.66°$, $A = 0°$, $k = 0.372$, and $M \simeq 0$.

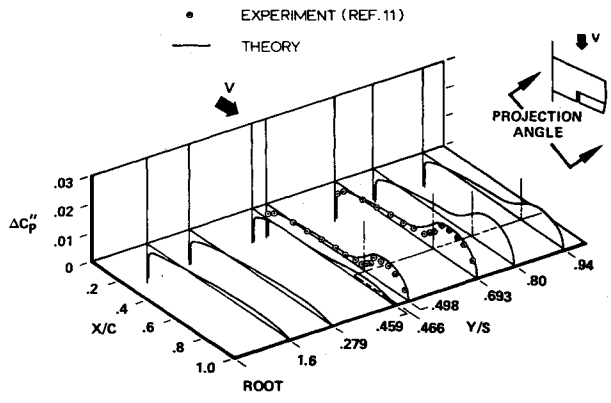


Fig. 12 Out-of-phase chordwise pressure distributions.

$$D_3(x,y) = -\frac{\beta^2}{2}\frac{\partial^2}{\partial\xi\,\partial\eta}\left[g_r(\xi,\eta)e^{-ik(x-\xi)}\right]_{\substack{\xi=x\\ \eta=y}} + ik\frac{\partial}{\partial\eta}\left[g_r(x,\eta)\right]_{\eta=y}$$

Numerical evaluation of the above downwash integrals is accomplished by subdividing the integration intervals into small regions and applying integration quadrature formulas appropriate to the function characteristics. Gaussian quadrature formulas containing unity, square-root, and logarithmic weight functions are extensively used in the integral evaluations.

## Theoretical-Experimental Comparisons

This section presents pressure distributions resulting from analysis of two wing-control surface configurations for which experimental data are available for comparison.

### Steady-State Results for a Partial-Span Flap Configuration

The partial-span control surface configuration shown in Fig. 8 represents the experimental planform of Ref. 10 to obtain chordwise pressure distributions due to a steady flap deflection. Pressures were obtained along a streamwise chord located at the 46% semispan station. The hingeline gap was sealed providing a one-to-one basis for comparing theoretical and experimental results.

Theoretical pressures were obtained along various streamwise chords spaced over the semispan and are shown in Fig. 9. The comparison indicates that the experimental pressures are accurately predicted by the theoretical technique over the length of the chordwise strip forward of the hingeline. The theoretical distribution over the control surface are only slightly larger than the experimental values.

### Unsteady Pressure Comparison

The side-by-side control surface configuration is shown in Fig. 10 for which unsteady pressures are obtained for various combination of flap deflections. The experimental model had small open gaps at the hingelines and at the side edges that will not provide a one-to-one basis in the comparison of the theoretical-experimental results in regions near the gaps.

Figures 11 and 12 present comparisons of theoretical and experimental pressure distributions for a mode shape in which the outer flap is oscillating and the inner flap and wing are maintained in a stationary position.

There is good agreement between the theoretical and experimental results in all areas except in localized regions near the hingelines. The experimental values are less than the theoretical values forward of the hingeline and slightly greater than the predicted values aft of the hingeline. The variations near the hingeline are attributed to open gap effects at the hingeline.

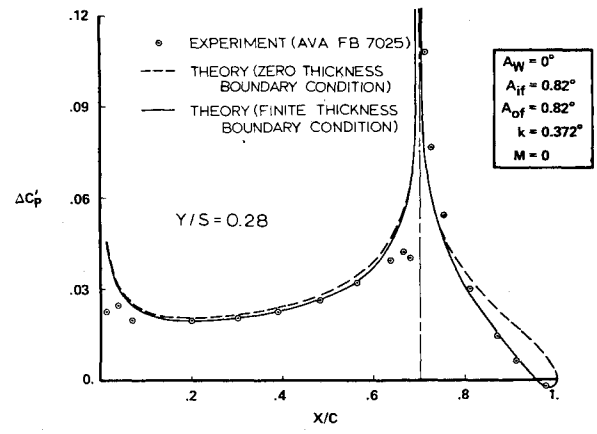


Fig. 13 In-phase pressure distributions predicted by zero thickness and finite thickness boundary conditions.

## Suggested Modification of Boundary Conditions

From an operational standpoint, it appears that if a local linearization is used, that is if the linearized boundary conditions $\bar{w}/V$ are modified to include local velocities due to airfoil thickness the resulting theoretical pressure distributions will simulate the physical flow conditions more accurately. That is, the boundary condition of the integral equation is obtained from the definition

$$\bar{W}_j(x,y,0) = \frac{1}{V}\frac{Dz}{Dt} = \frac{1}{V}\left[\frac{\partial z_j}{\partial t} + \frac{\partial z_j}{\partial x}\frac{\partial x}{\partial t}\right]$$

where $z_j$ represents the displacement of the sufface and is a function of time ($t$). $\partial x/\partial t$ is usually taken to be equal to the remote velocity $V$, and for a zero thickness airfoil section this may be correct. However, physical experiments are conducted on finite thickness airfoil sections having local velocities that are not uniform over the chord length. Consequently, the $\partial x/\partial t$ term should represent the local flow velocity $V_{\text{Local}}$ at collocation stations in making a comparison between theoretical and real flow results. $V_{\text{Local}}$ is defined as being the steady streamwise velocity distribution that differs from $V$ due to thickness effects only, and may be obtained from experimental results or by using the theoretical distributions of Ref. 12.

A numerical experiment was conducted to investigate the effects of local linearization on the pressure distributions. The experiment was conducted on configuration of Fig. 10 and using the ($V_{\text{Local}}/V$) distribution of Ref. 12 to modify the boundary conditions. Results of this investigation are presented in Fig. 13.

It appears that the pressure distributions obtained by the assumed mode approach using the preferred solution process and modifying the boundary conditions due to local velocities will provide predictions of the unsteady loadings that give reasonably good agreement with experimental results.

## References

[1]Rodden, W. P., Giesing, J. P., and Kálmán T. P., "New Developments and Applications of the Subsonic Doublet-Lattice Method for Nonplanar Configurations," AGARD symposium, Nov. 1970, Tonsberg, Norway.

[2]Berman, J. H., Skyppykevich, P., and Smedfield, J. B., "Unsteady Aerodynamic Forces in General Wing/Control Surface Configuration in Subsonic Flow," AFFDL-TR-67-117, May 1968, Air Force Flight Dynamics Lab., Wright-Patterson Air Force Base, Ohio.

[3]Landahl, M., "Pressure Loading Functions for Oscillating Wings with Control Surfaces," *AIAA Journal*, Vol. 6, No. 2, Feb. 1968, pp. 345–349.

[4]Ashley H., and Rowe, W. S., "Unsteady Aerodynamic Loading of Wings with Control Surfaces," *Z. Flugwissenschaften*, Vol. 18 Sept./Oct., 1970, pp. 321–330.

[5]Kussner H. G., "General Lifting Surface Theory," *Luftfahrtforschung*, Vol. 17, No. 11/12, Dec. 1940.

[6]Watkins, C. E., Runyan, H. L. and Woolston, D. S., "On the Kernel Function of the Integral Equation Relating the Lift and Downwash Distributions of Oscillating Finite Wings in Subsonic Flow," NACA Rep. 1234, 1955.

[7]Hsu P. T., "Calculation of Pressure Distributions for Oscillating Wings of Arbitrary Planform in Subsonic Flow by the Kernel Function Method," MIT ASRL T.R. 64-1, Oct. 1957.

[8]Multhopp, H., "Methods for Calculating the Lift Distribution of Wings (Subsonic Lifting-Surface Theory)," Aeronautical Research Council R-M 2884, Jan. 1950.

[9]Laschka B., "Zur Theorie der Harmonish Schwingenden Tragenden Flache bez Unterschallstromung," *Z. Flugwissenschaften*, Vol. 12, 1963, pp. 265–292.

[10]Hammond A. D. and Keffer B. A., "The Effect at High Subsonic Speeds of a Flap-Type Aileron on the Chordwise Pressure Distribution Near Midsemispan of a 35° Sweptback Wing of Aspect Ratio 4 having NACA 65A006 Airfoil Section," NACA RM L53C23, March 1953.

[11]Forsching, H., Triebstein, H., and Wagener J., "Pressure Measurements on Harmonically Oscillating swept Wing with Two Control Surfaces in Incompressible Flow," AVA FB 7025, 1970, AGARD Symposium, Tonsberg, Norway.

[12]Abbott I. H. and VonDoenhoff A. E., "Theory of Wing Sections," McGraw-Hill, New York, 1949.

JANUARY 1974 J. AIRCRAFT VOL. 11, NO. 1

# Flowfield Analysis for Successive Oblique Shock Wave-Turbulent Boundary-Layer Interactions

Chen-Chih Sun* and Morris E. Childs†
*University of Washington, Seattle, Wash.*

**A computation procedure is described for predicting the flowfields which develop when successive interactions between oblique shock waves and a turbulent boundary layer occur. Such interactions may occur, for example, in engine inlets for supersonic aircraft. Computations have been carried out for axisymmetric internal flows at $M_\infty = 3.82$ and 2.82. The effect of boundary layer bleed has been considered for the $M_\infty = 2.82$ flow. A control volume analysis is used to predict changes in the flow field across the interactions. Two bleed flow models have been considered. A turbulent boundary layer program has been used to compute changes in the boundary layer between the interactions. The results given are for flows with two shock wave interactions and for bleed at the second interaction site. In principle the method described may be extended to account for additional interactions. The predicted results are compared with measured results and are shown to be in good agreement when the bleed flow rate is low (on the order of 3% of the boundary layer mass flow), or when there is no bleed. As the bleed flow rate is increased, differences between the predicted and measured results become larger. Shortcomings of the bleed flow models at higher bleed flow rates are discussed.**

## Nomenclature

$A$ = $\{[(\gamma-1)/2]\, M_e^2/(T_w/T_e)\}^{1/2}$
$a$ = a constant in the wall-wake profile
$B$ = $\{(1+[(\gamma-1)/2]M_e^2)/(T_w/T_e)\} - 1$
$C$ = a constant in the Law of the Wall (usually equals 5.1)
$C_f$ = skin friction coefficient, $\tau_w/(1/2)\rho_e u_e^2$
$I_{Bx}$ = $x$-momentum of the bleed flow
$K$ = a constant in the Law of the Wall (usually equals 0.4)
$L$ = shock wave-boundary layer interaction length
$M$ = Mach number
$\dot{m}_B$ = boundary layer mass bleed rate
$P$ = pressure
$R$ = radial coordinate from tunnel centerline
$R_B$ = radial coordinate of dividing stream surface separating bleed flow from main flow, (see Fig. 3)
$Re$ = Reynolds number
$u$ = velocity in streamwise direction
$u^*$ = van Driest's generalized velocity, $(u_e/A)\arcsin\{[(2A^2u/u_e) - B]/(B^2+4A^2)^{1/2}\}$
$u_\tau$ = friction velocity, $(\tau_w/\rho_w)^{1/2}$
$x$ = axial coordinate, measured from shock generator tip
$y$ = coordinate normal to the tunnel wall
$\gamma$ = ratio of specific heats
$\Delta_E$ = a thickness of freestream flow to allow for boundary layer mass entrainment, (see Fig. 3)
$\delta$ = boundary layer thickness
$\delta^*$ = displacement thickness of the boundary layer
$\eta$ = $y/\delta$
$\theta$ = momentum thickness of the boundary layer
$\nu$ = kinematic viscosity
$\Pi$ = coefficient of the wake function
$\rho$ = mass density
$\sigma$ = $[(\gamma-1)/2]M_e^2/\{1+[(\gamma-1)/2]M_e^2\}$
$\tau$ = shear stress

*Subscripts*

$e$ = conditions at the edge of the boundary layer
$w$ = conditions at the wall
$\infty$ = freestream conditions ahead of the first interaction

Received April 23, 1973; revision received October 29, 1973. This work was supported by NASA Grant NGR-48-002-047 under administration of the Aerodynamics Branch, Ames Research Center.

Index categories: Boundary Layers and Convective Heat Transfer—Turbulent; Supersonic and Hypersonic Flow; Shock Waves and Detonations.

*Research Associate (Postdoctoral), Department of Mechanical Engineering.

†Professor of Mechanical Engineering. Member AIAA.

## Introduction

THE interaction of an oblique shock wave with a turbulent boundary layer is known to induce drastic changes in the boundary-layer properties and to cause substantial de-